

BIOCHEMICAL AND HISTOPATHOLOGICAL STUDY OF TOXICITY OF DIFFERENT SIZES OF SPHERICAL GOLD NANOPARTICLES ON NORMAL RATS - IN VIVO STUDY

Bothaina F Mahmoud¹, Iman A Sharaf¹, Amani H Kazem², Heba S Ramadan³, Ahmed F Taha¹

Department of Biochemistry¹ Department of Pathology² Department of Medical BioPhysics³
Medical Research Institute University of Alexandria

Accepted 5th March, 2014

ABSTRACT

Back ground: Gold nanoparticles (GNPs) offer a great promise in biomedicine. Currently, there is no data available regarding the toxicity of GNPs. ROS and free radical production is one of the primary mechanisms of nanoparticle toxicity. The present *in vivo* study investigated the toxicological effects of size-sorted GNPs along four different time intervals at the cellular levels that include liver, spleen and blood cells through biophysical and biochemical studies, these studies were confirmed by histopathological studies

Animals and Methods: Adult SpragueDewally male rats weighting (100-120g) received intraperitoneal injection of colloidal gold nanoparticles of different sizes (10,50,100nm) that were repeated day by day. Animals were scarified after (14,21,30 and 40) blood samples ,liver and spleen were collected. The parameters studied included: measuring of whole blood viscosity , RBCs aggregation parameters, hepatic lipid peroxidation, Super oxide dismutase (SOD), glutathione (GSH), glutathione disulfide (GSSG), GSH/GSSG ratio, glutathione redox potential (ΔE_G), and tumor necrosis factor-alpha (TNF- α) were measured in both liver homogenate and plasma of all studied and control groups. Histopathological examination of the liver and spleen were done .

Results: Significant increases were observed in all studied groups compared to controls in RBCs aggregation whole blood viscosities and liver lipid peroxidation, while significant decreases were noticed in hepatic SOD, GSH concentrations , GSH/GSSG ratio, glutathione redox potential (ΔE_G), and significant increase in hepatic and plasma TNF- α concentration of all studied groups after the four time intervals included in the present experiment. In all the studied parameters, the percentage of the increase or decrease was time dependant and was higher in 50nm group than 10nm and 100nm groups. The histopathological findings confirmed the biochemical alterations and revealed that, there were various degrees of hepatic tissue injury in the studied groups after the four time intervals of the experiment, characterized by mild to heavy inflammation, as well as necrosis and apoptosis. The spleen sections of GNPs-administrated rats revealed no significant differences in histology after 14 and 21 day of GNPs administration

Conclusion: *In vivo* cytotoxicity of size-sorted GNPs is the induction of oxidative stress and immune response. The toxicological effects of GNPs are time dependent. Different sizes of GNPs could be endocytosed by hepatic and splenic cells and have large toxic effect on hepatic tissue (apoptosis and necrosis) while its effect on splenic tissue is limited and could be observed after long-term repeated administration

KEYWORDS: Gold nanoparticle, Sizes, Rats, Oxidative stress, Antioxidant enzymes, cell death

1.0 INTRODUCTION

Nanotechnology can simply be defined as the technology at the scale of one-billionth of a meter. It is the design, characterization, synthesis and application of materials, structures, devices and systems by controlling shape and size at nanometer scale.^(1, 2)

Gold nanoparticles (GNPs) have gained increasing interest due to their special features, such as unusual optical and electronic properties, high stability and biological

compatibility, controllable morphology and size dispersion, and easy surface functionalization^(3, 4).

Gold and gold compounds are mainly applied as a drug for the treatment of rheumatic diseases including psoriasis, palindromic rheumatism, juvenile arthritis and discoid lupus erythematosus.^(5, 6)

Nanoparticles could have many adverse effects at the cellular level by interacting with vital cell components such as the membrane, mitochondria, or nucleus. Adverse outcomes could include organelle or DNA damage, oxidative stress, apoptosis (programmed cell death), mutagenesis, and protein up/ down regulation.^(7, 8)

Various in-vitro and in-vivo studies show that free radical formation can be triggered by nanoparticles.⁽⁹⁾ Nanoparticles can be taken up actively (phagocytosis) by certain cells (macrophages) and initiate ROS formation. Passive cellular uptake of particles has also been documented.^(10, 11)

Nanoparticles tend to form aggregations/agglomerations. It is unclear whether they can produce elevated ROS levels in this configuration. ROS can also develop directly on the surface of the particles, although this depends on particle structure. The overproduction or chronic production of ROS can cause inflammatory reactions, tissue changes and DNA, protein and lipid damage. Nanoparticles also cause mechanical damage within the cells and thus trigger oxidative stress.^(12, 13)

Oxidative damage to cellular DNA can lead to mutations and may, therefore, play an important role in the initiation and progression of multistage carcinogenesis.⁽¹⁴⁾ Nevertheless, high ROS concentrations induce apoptotic cell death in various cell types, suggesting that ROS contribute to cell death whenever they are generated in the context of the apoptotic process.^(15, 16)

Lipid peroxidation (LPO) changes molecule characteristics, making it more hydrophilic; this can alter structure and function of the membrane. The LPO products such as aldehydes (malondialdehyde and hydroxynonenal), are capable of forming crosslinks with lipids, proteins and nucleic acids, thereby causing damage to the macromolecules, which are essential components of biological tissues.⁽¹⁷⁾

Antioxidants can neutralize the free radicals through homeostatic activity of the cells. The main enzymatic "scavengers" responsible for the prevention of ROS formation and oxidation are superoxide dismutase, catalase and glutathione peroxidase.⁽¹⁸⁾ Superoxide dismutase enzyme converts superoxide radical anion into hydrogen peroxide (H₂O₂). Hydrogen peroxide is a weak oxidant attacking mainly thiols.⁽¹⁹⁾

Glutathione (GSH) is among the most important antioxidants in cells, being used in enzymatic reactions to eliminate peroxides and in nonenzymatic reactions to maintain ascorbate and α -tocopherol in their reduced and functional forms. In these reactions, GSH is converted to its disulfide form, GSSG. The most widely used indicator of the redox state of the GSH pool is the ratio of reduced glutathione (GSH) to oxidized glutathione (GSSG).⁽²⁰⁾

Glutathione oxidation precedes nuclear DNA fragmentation. These signs of oxidative stress are caused, at least in part, by an increase in peroxide production by mitochondria from apoptotic cells.⁽²¹⁾

Nanoparticles could also be identified as foreign by the immune cells, causing the cells to react against either surface or core components to mount an inflammatory response, which involve secretion of signaling molecules (known as cytokines such as TNF- α) to attract more cells to destroy the foreign substances.⁽¹⁰⁾

2.0 Study Objectives

The present study aimed to evaluate from the biochemical, biophysical and histopathological points of view the toxicological effects of different sizes of colloidal gold nanoparticles administered intraperitoneally to normal adult male rats.

3.0 MATERIALS AND METHODS

3.1 Experimental animals and their groups:

The experiments were carried out on 140 male Sprague-Dewally rats of mean weight 100-120g (purchased from Faculty of Medicine, Alexandria University, animal house). Each four animals were housed in a cage in a wellventilated room (25 light: dark cycle at the animal house. The animals were acclimated to the environment for at least two weeks before onset of the experiments. The design of the study was in accordance with the ethical guide lines prescribed by the Medical Research Institute.

After 1 week of acclimatization, the animals were randomly divided into 3 main experimental groups (n=40/gp)

Groups (I,II,III) were injected intraperitoneally with a suspension of gold nanoparticles of about 10nm, 50nm, 100nm at a dose of 1ml (1mM)/200gm (animal weight) respectively and **group IV** consists of twenty normal male rats that were injected intraperitoneally with saline only and serve as control group.

Animals sacrificed after 14, 21, 30 and 40 days of repeated administration- day by day- of size sorted GNPs. At time of sacrifice, animals were anaesthetized by light ether.

Blood samples were collected from dorsal vein on EDTA coated tubes for determination of red blood cells aggregation and plasma TNF- α .

3.2 Tissue samples

As fast as possible, a biopsy of liver was excised from animals and blood was removed by perfusing the tissue with a cold phosphate buffer saline (pH=7.4, 0.1M). The biopsy was weighed and homogenized in phosphate buffer saline (pH=7.4, 0.1M) to make up 1 to 5 W/ V final preparation. The whole homogenate was centrifuged at 1600 rpm for 20 min at 5 oC, the supernatant was immediately stored at -20 oC for further use.

Also, another biopsy of liver and spleen tissues was dissected and preserved in 10% formalin for preparation of microscopic sections and exploring morphological changes.

3.3 Biophysical studies

3.3.1 Preparation of gold nanoparticles:⁽²²⁾

Gold nanoparticles were prepared using citrate ions which acts as a reducing and a capping agent. This formation of gold nanoparticles can be observed by a change in color since small nanoparticles of gold are red. The presence of this colloidal suspension can be detected by the reflection of a laser beam from the particles.

3.3.2 Characterization of Gold Nanoparticles⁽²³⁻²⁵⁾

3.3.2.1 Particle size distribution

The particle size distribution of the gold nanoparticles was determined by laser light scattering on a Beckman Coulter Particle Size Analyzer (N5 submicron particle size analyzer, Japan).

The shape of prepared nanoparticles was determined by Transmission Electron Microscope (Jeol, JSM-6360LA, Japan) after mounting them on carbon coated copper grids and stained with uranyl acetate (SPI-Module™ sputter coater, Japan).

3.3.3 Aggregation shape parameter (ASP):

After the Scion program counted each groups and calculated the area and perimeter of each count, the data was entered into an Excel program sheet in order to calculate the ASP for each count, which was calculated using the following formula⁽²⁶⁾:

$$ASP = 4 \pi A / P^2$$

Where:

A is the projected area of the aggregate,
P is the perimeter of the project

3.3.4 Determination of whole blood viscosity ⁽²⁷⁾

A wells-Brookfield Cone/Plate LVDV-II+ viscometer with a CP-40 cone (Brook field laboratories, Japan) coupled to a refrigerated recirculating fluid path to control the temperature of the sample (Cole Parmer, Vernon Hills, IL) was used to measure the viscosity over a range of different shear rates

3.4 Biochemical studies

3.4.1 Determination of lipid peroxidation:

Malondialdehyde in whole liver homogenate was determined according to the method of Draper and Hadley. (28) The sample under test was heated with thiobarbituric acid (TBA) at low pH. The resulting pink chromogen has a maximal absorbance at 532nm

3.4.2 Determination of superoxide dismutase (SOD) activity:

was done by pyrogallol method of Marklund and Marklund.⁽²⁹⁾ The method depends on the spontaneous autoxidation of pyrogallol at alkaline pH, resulting in the production of superoxide anion radicals (O₂⁻), which in turn enhance autoxidation of pyrogallol. Autoxidation is manifested as an increase in absorbance at 420 nm.

3.4.3 Determination of glutathione and glutathione disulfide in liver homogenate:

was done by the enzymatic method described by Griffith et al⁽³⁰⁾ The method depends on the oxidation of GSH by 5, 5-dithiobis-(2-nitrobenzoic acid) (DTNB) to yield GSSG and 5-thio-2-nitrobenzoic acid (TNB). Oxidized GSSG is reduced enzymatically by the action of glutathione reductase and NADPH to regenerate GSH which reacts again. The rate of TNB formation is monitored at 412 nm and is proportional to the sum of GSH and GSSG (tGSH) present in the sample:

The GSSG content is determined by the same assay as total glutathione, but the reduced glutathione is bound by 2-vinylpyridine. The GSSG content in the samples were determined from a standard curve. Results were subsequently expressed as nmol /mg protein.

Reduced glutathione was obtained by subtracting the values of oxidized glutathione (GSSG) from the values of total glutathione (tGSH):

$$rGSH = tGSH - GSSG$$

The most widely used indicator of the redox state of the cells is the ratio of reduced glutathione (rGSH) to oxidized glutathione (GSSG).⁽²⁰⁾

3.4.4 Calculation of redox potential ⁽³¹⁾

Redox state is a term that describes the ratio of the oxidized and reduced form of a specific redox couple. The redox state

of a redox couple is defined by the half-cell reduction potential and the reducing capacity of that couple.

The reducing capacity would be estimated by determining the concentration of the reduced species in the redox couple, the reduction potential can be estimated with the Nernst equation, which is written as:

$$\Delta E = \Delta E_0 - [59.1/n] \log Q$$

Where:

ΔE :is the reduction potential or electromotive force

ΔE_0 : is the electromotive force under standard conditions.

n: Is the number of electrons in the reaction.

Q: is the mass action expression for the redox equation;

3.5 Determination of total protein in the sample by the method of Lowry et al. ⁽³²⁾.

3.5.1 Quantitative detection of rat plasma and liver TNF- α by ELISA kit ⁽³³⁾

A colored product is formed in proportion to the amount of rat TNF- α present in the sample or the standard. The reaction is determined by addition of acid and absorbance is measured at 450 nm. A standard curve is prepared from 7 rats TNF- α standard dilutions and rat plasma TNF- α sample concentration determined

3.6 Histopathological study

3.6.1 Light microscopic examination

Liver and spleen samples were excised from rats of each group and preserved in a 10% formalin solution for histopathological study. The fixed tissues were embedded in paraffin; sections 3-5 μ m thick were obtained, deparaffinized, dehydrated in ethanol (50-100%), and cleared with xylene. The extent of GNPs-induced cytotoxicity, including inflammation, cell apoptosis, cell necrosis, steatosis and others was evaluated by assessing the morphological changes in liver and spleen sections stained with hematoxylin and eosin (H&E) under light microscope.⁽³⁴⁾

3.7 Statistical analysis of the data⁽³⁵⁾

Data were analyzed using SPSS software package version 18.0 (SPSS, Chicago, IL, USA). Test of normality was applied on the data by using Kolmogorov-Smirnov test, Shapiro-Wilk test, 7 and also D'Agstino. Quantitative data were expressed using range, mean, standard deviation and median.

Quantitative data were analyzed using F-test (ANOVA) to compare the three categories of outcome. Non-normally distributed quantitative data were analyzed using Mann Whitney test for comparing two groups while for more than two groups Kruskal Wallis test was applied. Pearson coefficient was used to analyze correlation between any two variables. The p value was assumed to be significant at 0.05.

4.0 RESULT

4.1 Biophysical studies:

4.1.1 Preparation and characterization of size-sorted GNP

Particle size distribution that was carried out by particle size analyzer showed preparation of gold nanoparticles with mean particle sizes of 10.4nm, 53.3nm and 103.1nm with baseline error of 3.29%, 1.34% and 0.22% respectively at

diffraction angle of 11.1 °. These results are presented in Figures 1-3 respectively.

The findings obtained from transmission electron microscopy examination revealed the presence of completely spherical GNPs with smooth surfaces that have sizes in the range of 10nm, 50nm and 100nm. These results are shown in Figures 4 –6 respectively.

**11.1°, Repetition 1 Unimodal Distribution
Unimodal Results Summary**

Angle	Mean (nm)	P.I.	Diff.Coeff (m ² /s)	Counts/s	Baseline Error	Overflow
11.1°	10.4	0.707	4.13e-11	1.31e+06	3.29%	0

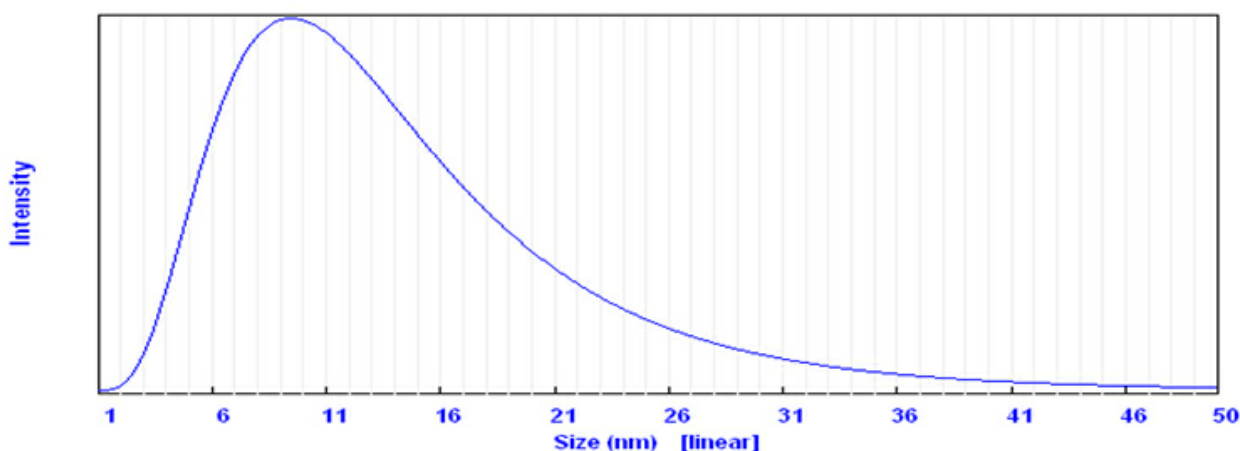


Fig. (1): Particle size distribution of prepared gold nanoparticles showing mean particle size of 10.4nm at diffraction angle of 11.1°.

**11.1°, Repetition 1 Unimodal Distribution
Unimodal Results Summary**

Angle	Mean (nm)	P.I.	Diff.Coeff (m ² /s)	Counts/s	Baseline Error	Overflow
11.1°	53.3	-5.635	8.04e-12	2.47e+06	1.34%	0

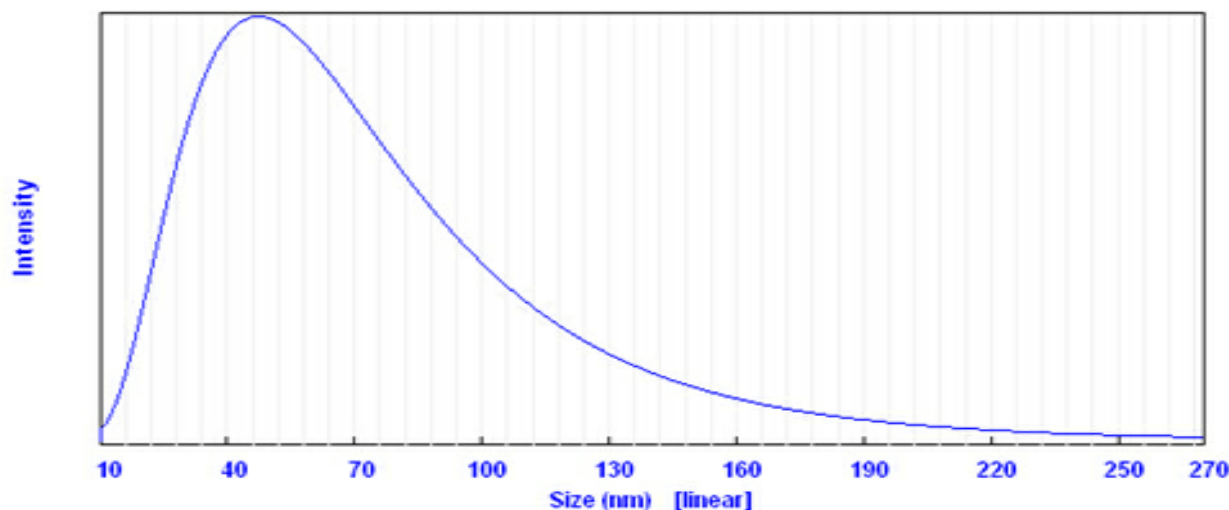


Fig. (2): Particle size distribution of prepared gold nanoparticles showing mean particle size of 53.3nm at diffraction angle of 11.1°.

Different Angle Unimodal Distribution Results for Repetition 1
Unimodal Results Summary

Angle	Mean (nm)	P.I.	Diff.Coeff (m ² /s)	Counts/s	Baseline Error	Overflow
11.1°	103.1	0.873	4.16e-12	9.28e+05	0.22%	0
90.0°	84.9	0.991	5.05e-12	1.29e+06	5.60%	0

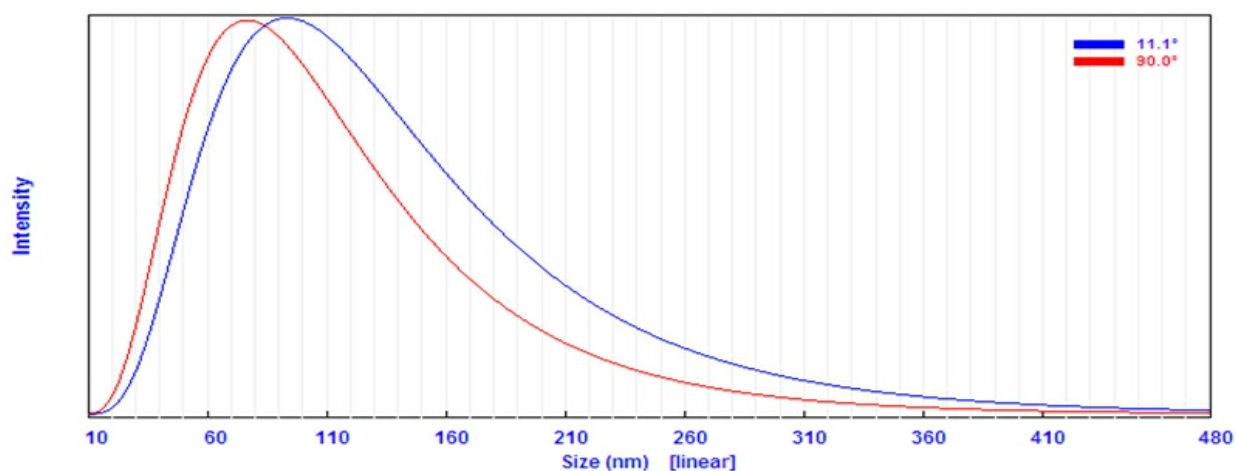


Fig. (3): Particle size distribution of prepared gold nanoparticles showing mean particle size of 103.1 nm at diffraction angle of 11.1°.

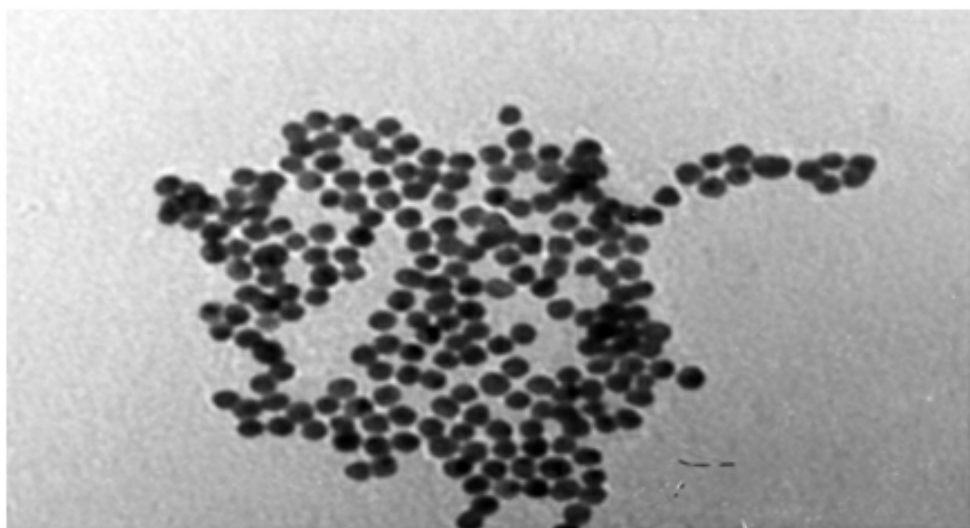


Fig. (4): TEM of spherical GNPs with an average size of 10nm. (Mag. 35000x)

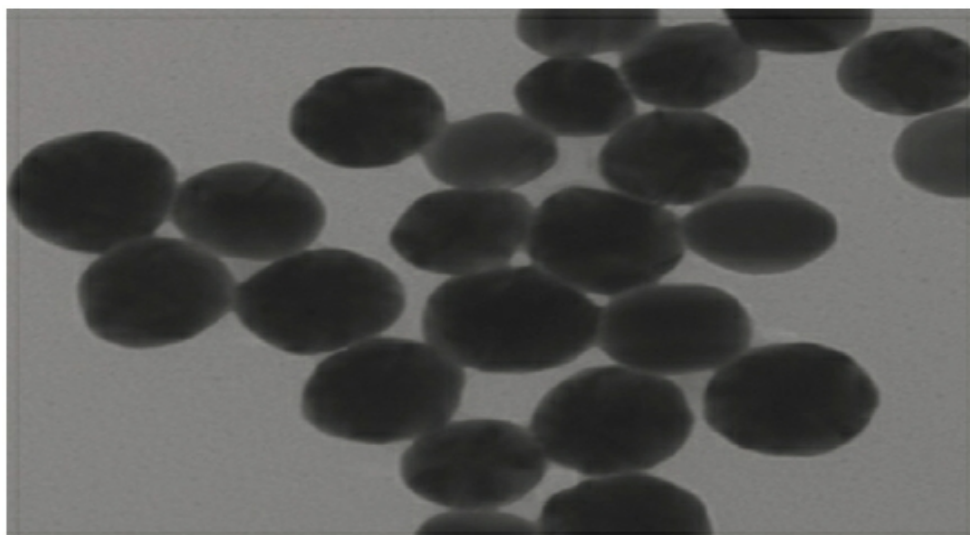


Fig. (5): TEM of spherical GNPs with an average size of 50nm (Mag. 50000x)

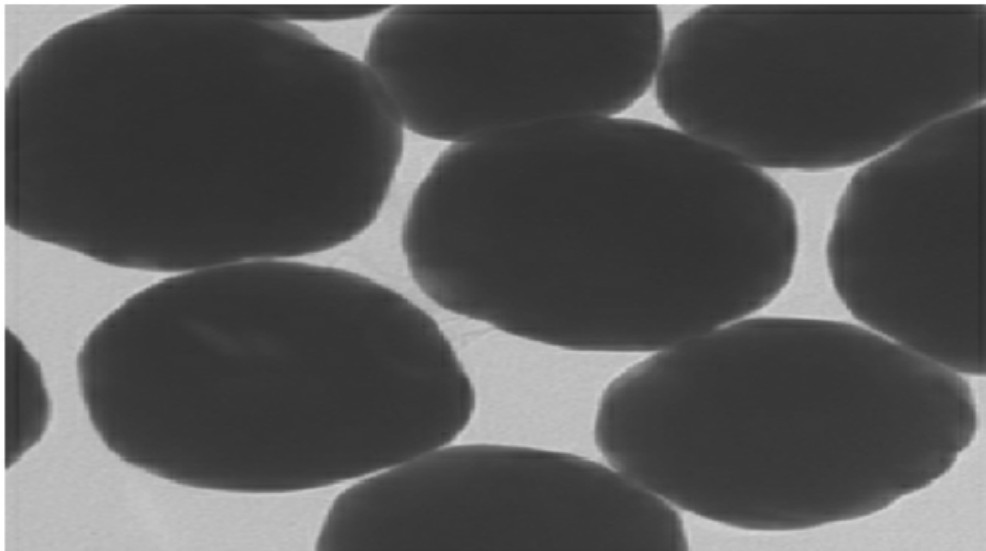


Fig. (6): TEM of spherical GNPs with an average size of 100nm. (Mag. 55000x)

Statistical analysis of aggregation shape parameter (ASP) and blood viscosity values of studied and control groups are presented in (Table 1).

After 14 days of repeated administration of different sizes of gold nanoparticles, the results showed that 100nm group exhibited a non-significant ($p > 0.05$) increase in ASP by about 3.26% compared to control group. While, 50nm group and 10nm group exhibited a significant ($p < 0.05$) increase in ASP by about 11.31%, 7.99 % respectively.

The data obtained also showed that, after 21, 30 and 40 days of repeated administration of size-sorted gold nanoparticles, there were marked significant ($p < 0.05$) increase in ASP in all studied groups that included 100nm, 50nm and 10nm groups.

The absolute viscosity of blood was measured for both controls and studied groups over a wide range of shear rates at all times intervals included in this experiment (Table 1).

The results showed that, in all studied groups, non-significant ($p > 0.05$) increase in blood viscosity was shown after 14 days of administration of different sizes of gold nanoparticles, while, after 21, 30 and 40 days of repeated administration of size-sorted gold nanoparticles, the studied groups showed marked significant ($p < 0.05$) increase in blood viscosity compared to controls. The presented data revealed that, in each time interval, the percentage of the increase in ASP values and whole blood viscosity were higher in 50nm group than in both 10nm and 100nm groups and were directly proportional with the time of administration.

Table 1: Statistical analysis of aggregation shape parameters (ASP) and whole blood viscosity (cP) of studied groups compared to control group in each time interval

Biophysical parameters	days Of sacrifice	Control	100 nm	50 nm	10 nm	^{KW}p
ASP	14	0.63 ± 0.03	0.65 ± 0.02	0.70@# ± 0.03	0.68@ ± 0.03	0.002*
	21	0.65 ± 0.02	0.72@ ± 0.02	0.79@# ± 0.02	0.74@\$ ± 0.04	<0.00 1*
	30	0.62 ± 0.02	0.75@ ± 0.05	0.81@# ± 0.02	0.76@\$ ± 0.02	<0.00 1*
	40	0.65 ± 0.03	0.76@ ± 0.03	0.83@# ± 0.03	0.77@\$ ± 0.02	<0.00 1*
cP	14	10.16±0.1 5	10.16±0.13	10.20±0.21	10.22±0.15	0.938
	21	10.34±0.1 3	11.22@±0.5 7	12.36@#±0.6 7	11.86@±0.46	0.002*
	30	10.40±0.1 2	11.34@±0.5 4	12.78@#±0.3 8	12.04@#±0.4 5	0.001*
	40	10.38±0.1 9	11.48@±0.5 8	13.38@#±0.8 1	12.82@#±0.4 0	0.001*

(Values expressed as Mean±SD)

^{KW}p : p value for Kruskal Wallis test

@: p value for Mann Whitney test between control and each other groups

#: p value for Mann Whitney test between 100 nm group and each other groups

\$: p value for Mann Whitney test between 50 nm and 10 nm group

*: Statistically significant at $p \leq 0.05$

4.2 Biochemical studies:

Hepatic malondialdehyde levels, SOD, tGSH, rGSH, rGSH / GSSG ratio and glutathione redox potential (ΔEG) in controls

and different studied groups are illustrated in (Table 2.).

The data obtained showed that after the four time intervals included in the present experiment, there were marked

significant ($p \leq 0.05$) increase in MDA levels in all studied groups which includes 100nm, 50nm and 10nm groups.

There were marked significant ($p \leq 0.05$) decrease in SOD, tGSH, GSH, decrease in GSH / GSSG ratio, and also there was a marked significant ($p \leq 0.05$) decrease in glutathione redox potential (ΔE_G) values in the liver of all studied groups compared to controls. Plasma and liver TNF- α concentrations are illustrated in (Table 3).

The data showed that after the four time intervals included in the study, there were marked significant ($p \leq 0.05$) increase in all studied groups compared to controls.

The data of all studied parameters revealed that, in each time interval, the percentage of change in 50nm group was higher than in both 10nm and 100nm groups and was directly proportional to the time of administration.

Table 2: Values of Hepatic malondialdehyde, SOD, tGSH, rGSH, rGSH / GSSG ratio and glutathione redox potential (ΔE_G) of all studied groups compared to control group in each time interval

Biophysical parameters	Day of scarification	Control	100 nm	50 nm	10 nm	P
MDA (nmole/mg protein)	14	1.02 \pm 0.16	7.0@ \pm 0.68	9.23@# \pm 0.35	8.71@#\$ \pm 0.46	<0.001*
	21	1.19 \pm 0.21	9.9@ \pm 0.15	11.23@## \pm 0.35	10.67@## \pm 0.34	<0.001*
	30	1.40 \pm 0.16	11.91@ \pm 0.34	12.86@## \pm 0.21	12.31@#\$ \pm 0.31	<0.001*
	40	1.94 \pm 0.35	13.22@ \pm 0.24	14.24@## \pm 0.21	13.69@#\$ \pm 0.32	<0.001*
SOD (U/min/mg prot)	14	41.11 \pm 1.46	34.76 ^a \pm 0.69	29.84 ^{ab} \pm 0.64	31.59 ^{ab} \pm 0.96	<0.001*
	21	39.29 \pm 1.36	29.73 ^a \pm 0.59	26.35 ^{ab} \pm 0.61	28.11 ^{abc} \pm 0.52	<0.001*
	30	37.69 \pm 0.56	26.25 ^a \pm 0.59	22.02 ^{ab} \pm 0.81	24.47 ^{abc} \pm 0.57	<0.001*
	40	37.17 \pm 0.92	21.64 ^a \pm 1.10	17.30 ^{ab} \pm 0.64	19.33 ^{abc} \pm 0.53	<0.001*
TGTH (nmole/mg prot)	14	50.16 \pm 3.09	40.72@ \pm 19.97	35.12@# \pm 1.49	40.15@#\$ \pm 1.88	<0.001*
	21	43.74 \pm 2.90	27.85@ \pm 1.13	22.57@# \pm 1.24	24.61@#\$ \pm 1.76	0.002*
	30	40.22 \pm 2.08	16.12@ \pm 0.94	11.16@# \pm 0.052	13.40@#\$ \pm 0.80	<0.001*
	40	37.02 \pm 3.15	10.0@ \pm 0.54	7.89@# \pm 0.50	8.86@#\$ \pm 0.29	<0.001*
GSSG (nmole/mg prot)	14	9.72 \pm 0.65	12.65@ \pm 0.66	12.61@# \pm 0.58	3.45@#\$ \pm 0.66	<0.001*
	21	8.90 \pm 0.56	10.18@ \pm 0.45	9.22# \pm 0.58	9.65 \pm 0.89	18.883*
	30	8.86 \pm 0.52	7.05@ \pm 0.39	5.35@# \pm 0.26	6.13@#\$ \pm 0.37	13.939*
	40	8.17 \pm 0.64	4.89@ \pm 0.39	4.30@# \pm 0.30	4.69@#\$ \pm 0.15	29.696*
rGSH (nmole/mg prot)	14	40.44 \pm 2.47	28.11@ \pm 1.37	22.65@# \pm 0.97	26.66@#\$ \pm 1.18	21.482*
	21	34.84 \pm 2.37	17.66@ \pm 0.70	13.35@# \pm 0.70	14.96@#\$ \pm 0.96	<0.001*
	30	31.36 \pm 1.65	9.07@ \pm 0.56	5.82@# \pm 0.27	7.27@#\$ \pm 0.44	<0.001*
	40	28.86 \pm 2.53	5.10@ \pm 0.36	3.59@# \pm 0.21	4.18@#\$ \pm 0.16	<0.001*
rGSH/GSSG ratio	14	4.15 \pm 0.08	2.22@ \pm 0.06	1.79@# \pm 0.03	1.98@#\$ \pm 0.03	31.592*
	21	3.91 \pm 0.10	1.73@ \pm 0.03	1.46@# \pm 0.03	1.55@#\$ \pm 0.08	29.879*
	30	3.54 \pm 0.13	1.28@ \pm 0.02	1.09@# \pm 0.02	1.18@#\$ \pm 0.02	31.596*
	40	3.53 \pm 0.08	1.09@ \pm 0.11	0.83@# \pm 0.02	0.89@#\$ \pm 0.02	31.501*
ΔE_G (-mV)	14	167.62 \pm 0.81	156.51@ \pm 1.21	149.51@# \pm 1.64	152.51@#\$ \pm 1.55	29.912*
	21	165.64 \pm 0.54	147.55@ \pm 2.24	138.90@## \pm 2.34	142.47@#\$ \pm 2.14	28.843*
	30	162.83 \pm 0.52	137.03@ \pm 0.99	130.16@# \pm 1.59	133.13@#\$ \pm 1.40	29.833*
	40	161.76 \pm 0.75	128.52@ \pm 2.29	120.39@# \pm 2.27	123.61@#\$ \pm 3.68	26.868*

(Values expressed as Mean \pm SD)

^{KW}p: p value for KruskalWallis < 0.001*

@: Mann Whitney test between control and each other groups

#: Mann Whitney test between 100 nm group and each other groups

\$: Mann Whitney test between 50 nm and 10 nm group

*: Statistically significant at $p \leq 0.05$

p: p value of test (ANOVA)

a: p value of Post Hoc test (LSD) between control and each other groups

b: p value of Post Hoc test (LSD) between 100 nm group and each other groups

c: p value of Post Hoc test (LSD) between 50 nm and 10 nm group

*: Statistically significant at $p \leq 0.05$

Table 3 : TNF- α values in plasma and liver samples of controls and different study groups

Biochemical parameters	Day of scarification	Control	100 nm	50 nm	10 nm	KWp
Plasma TNF- α Values (pg/ml)	14 day	41.40 \pm 3.97	78.10@#\$ \pm 2.77	91.10# \pm 2.92	84.0 \pm 3.33	0.010*
	21 day	43.0 \pm 3.81	95.30@ \pm 3.37	109.20@# \pm 3.3	104.20@#\$ \pm 3.29	<0.001*
	30 day	455.80 \pm 5.0	112.80@ \pm 3.71	125.20@# \pm 3.55	120.60@#\$ \pm 3.50	<0.001*
	40day	48.60 \pm 4.39	131.20@ \pm 3.61	143.20@# \pm 1.81	38.30@#\$ \pm 1.42	<0.001*
Hepatic TNF- α Values (pg/ml)	14 day	164.60 \pm 4.3	381.40@ \pm 2.80	404.40@# \pm 3.03	394.10@#\$ \pm 1.60	<0.001*
	21 day	168.8 \pm 4.0	409.0@ \pm 1.56	431.60@# \pm 2.99	423.50@#\$ \pm 2.22	<0.001*
	30 day	173.20 \pm 4.0	439.50@ \pm 2.27	460.60@# \pm 2.50	452.50@#\$ \pm 1.08	<0.001*
	40 day	176.60 \pm 4.8	468.50@ \pm 2.68	487.90@# \pm 3.28	478.70@#\$ \pm 3.40	<0.001*

(Values expressed as mean \pm SD)

KWp: p value for Kruskal

@: p value for Mann Whitney test between control and each other groups

#: p value for Mann Whitney test between 100 nm group and each other groups

\$: p value for Mann Whitney test between 50 nm and 10 nm group

*: Statistically significant at $p \leq 0.05$

4.3 Correlation between glutathione redox potential and hepatic TNF- α in the 50nm group

redox potential and hepatic TNF- α after 21, 30 and 40 days, respectively, of repeated administration of 50nm GNPs. (Fig. 7, 8, and 9).

4.4 Histopathological study

The histopathology of liver and spleen sections of all studied and control groups after the four time intervals of the experiment are presented in Figures (10—17). The hepatic tissue sections of studied animals revealed various degrees of hepatic tissue injury after the four time intervals of the experiment, characterized by mild to heavy portal and lobular inflammation, hepatocellular degeneration, and fatty changes (steatosis).

The histopathological examination revealed that there were

two types of liver cell death, apoptosis (or programmed cell death) and necrosis (or sudden cell death).

Also, it was observed that necrotic foci were often associated with fibrosis. On the other hand, the splenic tissue sections of GNPs-administrated rats revealed no significant differences in histology after 14 day and 21 day of GNPs administration.

Some morphological changes that include congested red pulp, reactive white pulp and wide reactive marginal zone were observed after 30day and 40 day of GNPs administration.

It was noticed that the recorded abnormal morphological changes in both the hepatic and splenic tissue sections increased with increasing time of administration. In each time interval, the recorded destructive and degenerative changes were maximum at 50nm GNPs administrated rats.

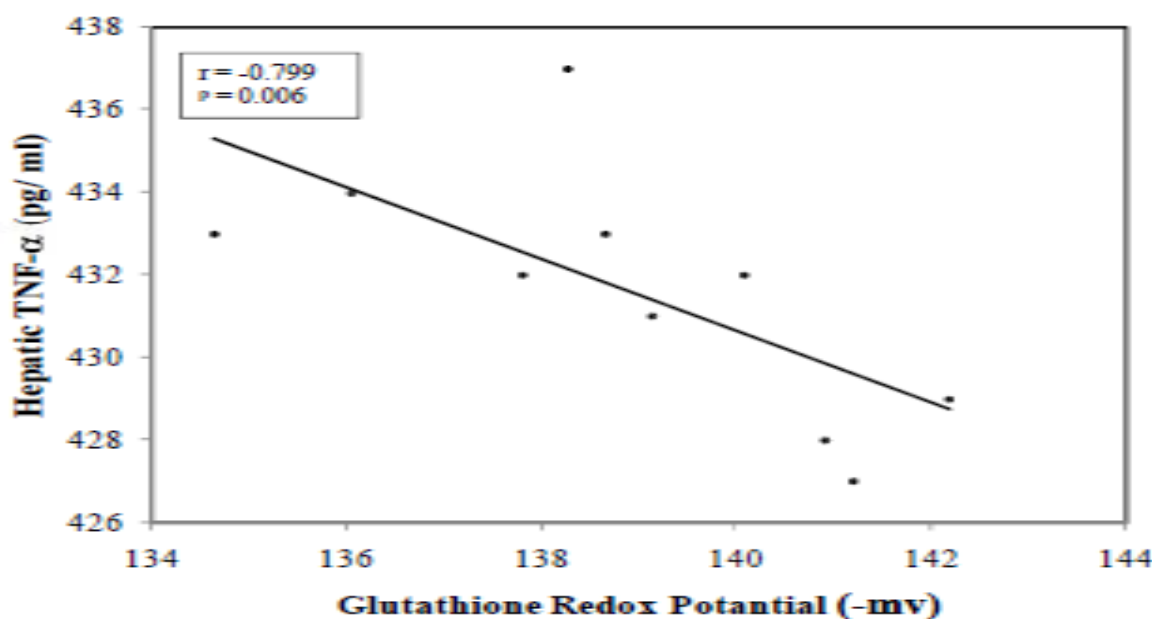


Fig. (7): Correlation between glutathione redox potential and hepatic TNF- α after 21 day of repeated administration of 50nm GNPs

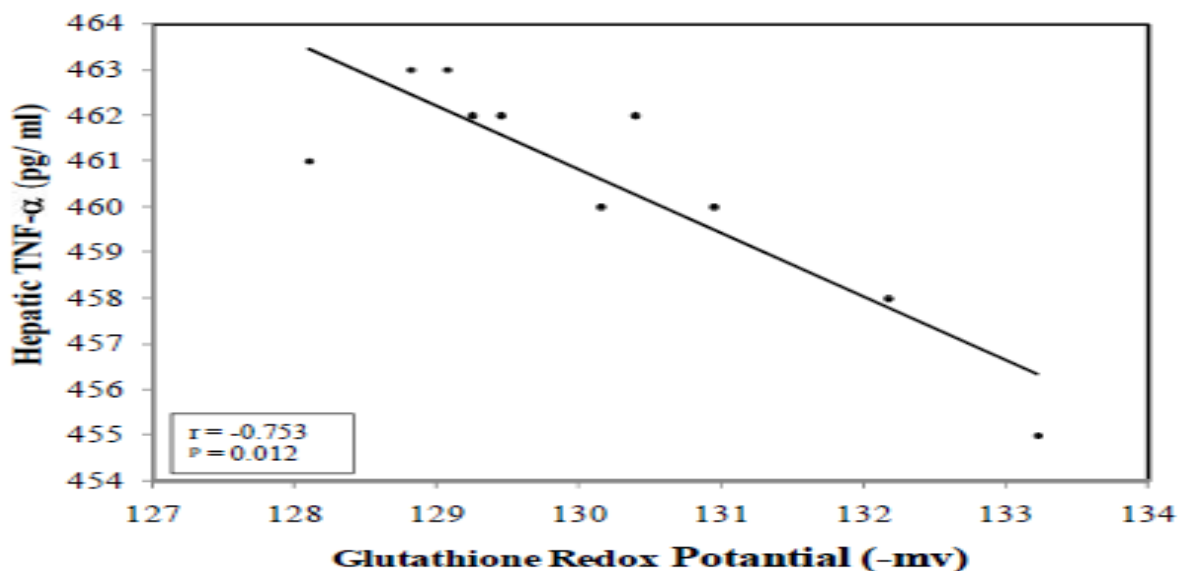


Fig. (8): Correlation between glutathione redox potential and hepatic TNF-α after 30 day of repeated administration of 50nm GNPs

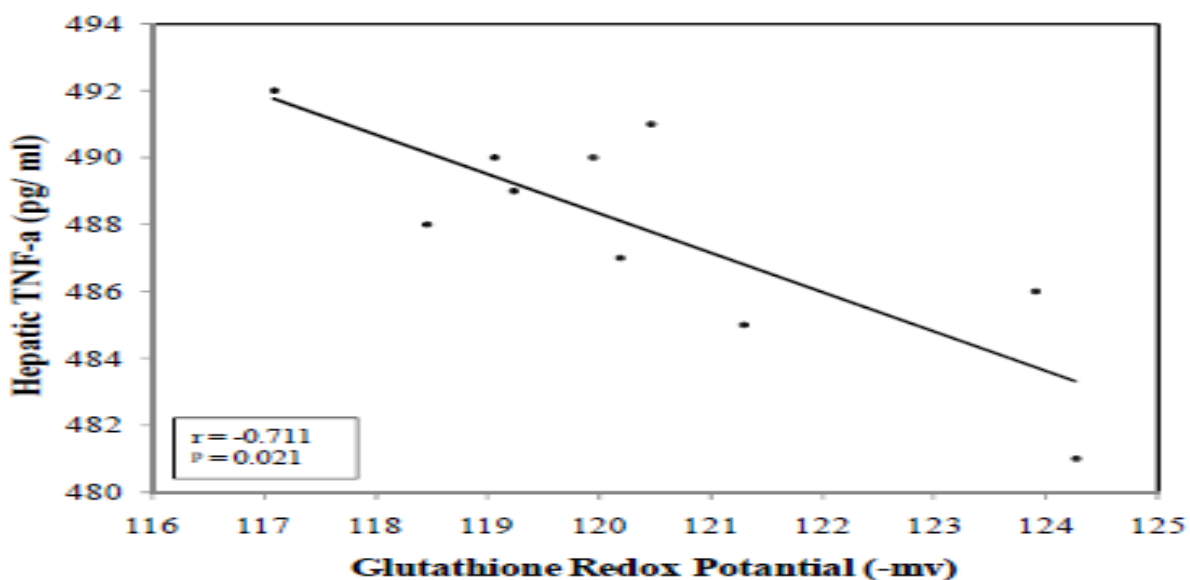
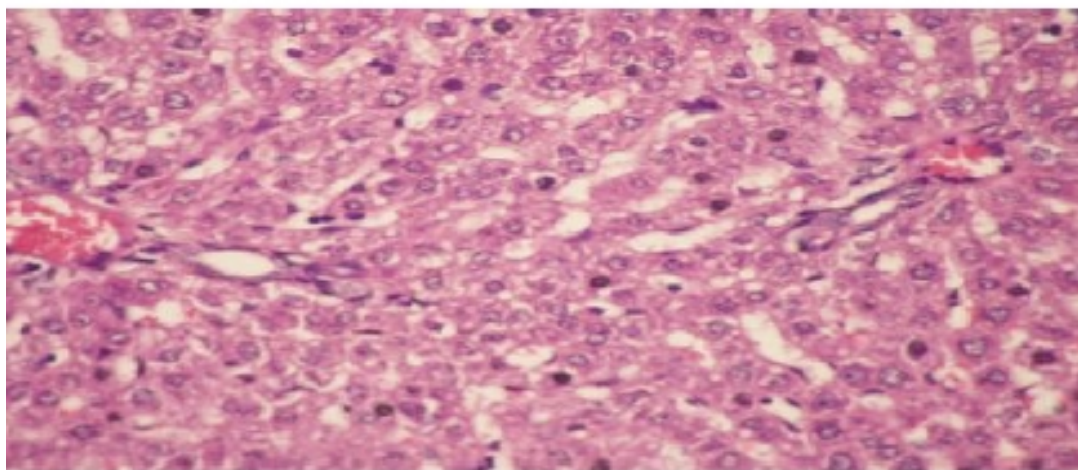
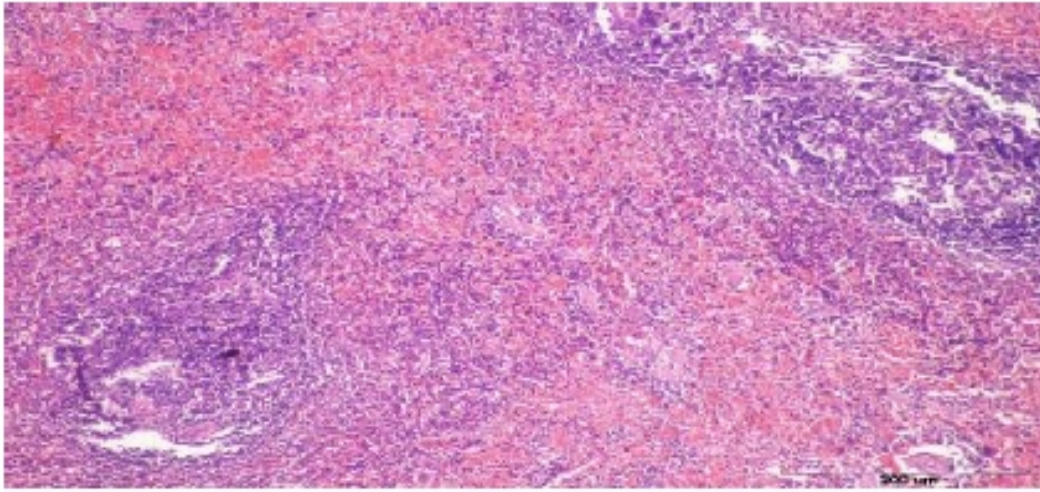


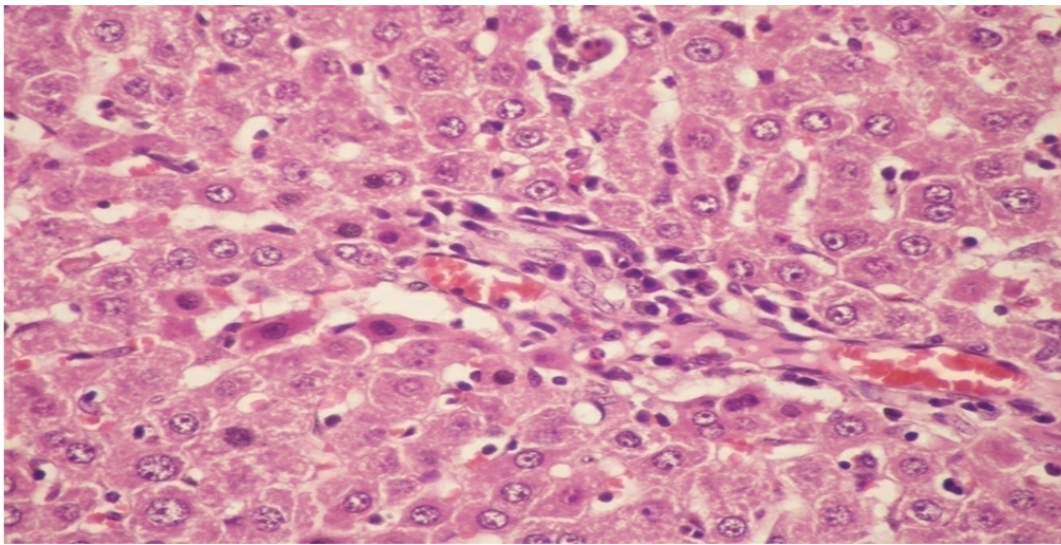
Fig. (9): Correlation between glutathione redox potential and hepatic TNF-α after 40 day of repeated administration of 50nm GNPs



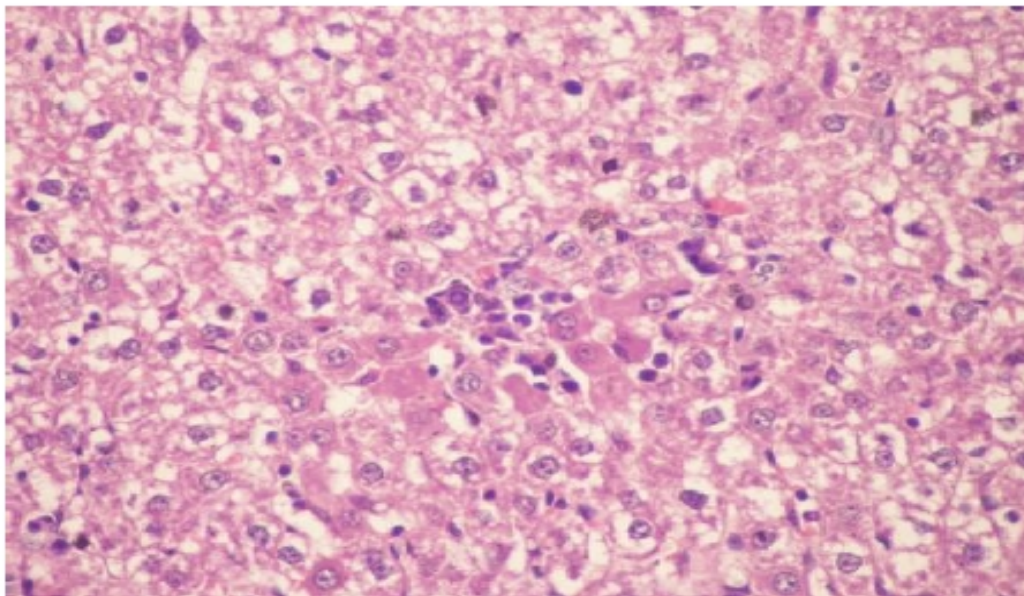
Fig(10): Hepatic tissue section showing normal liver architecture. (X400)



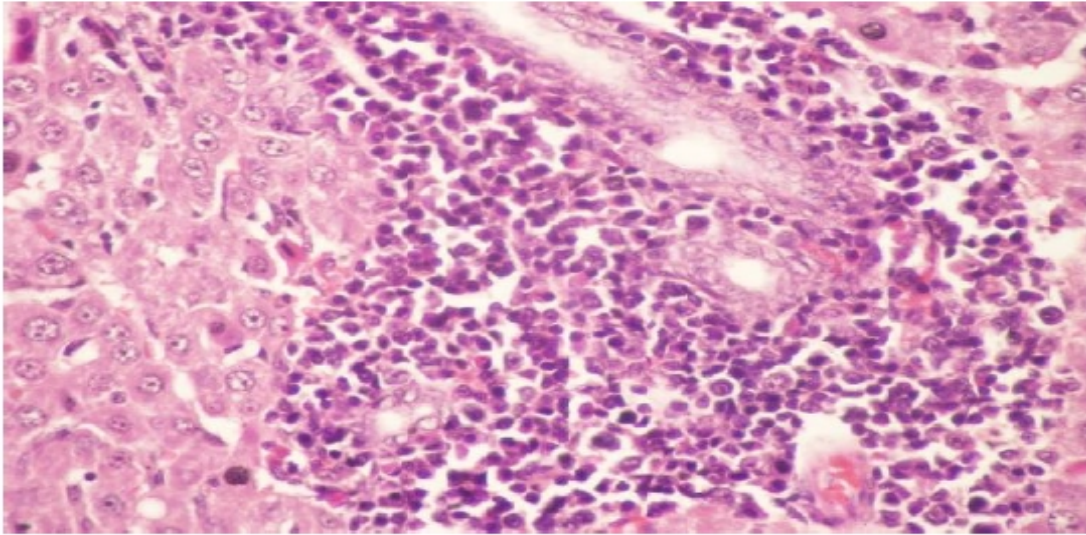
Fig(11): H&E stained splenic tissue section showing normal splenic architecture (normal white and red pulp). (x200)



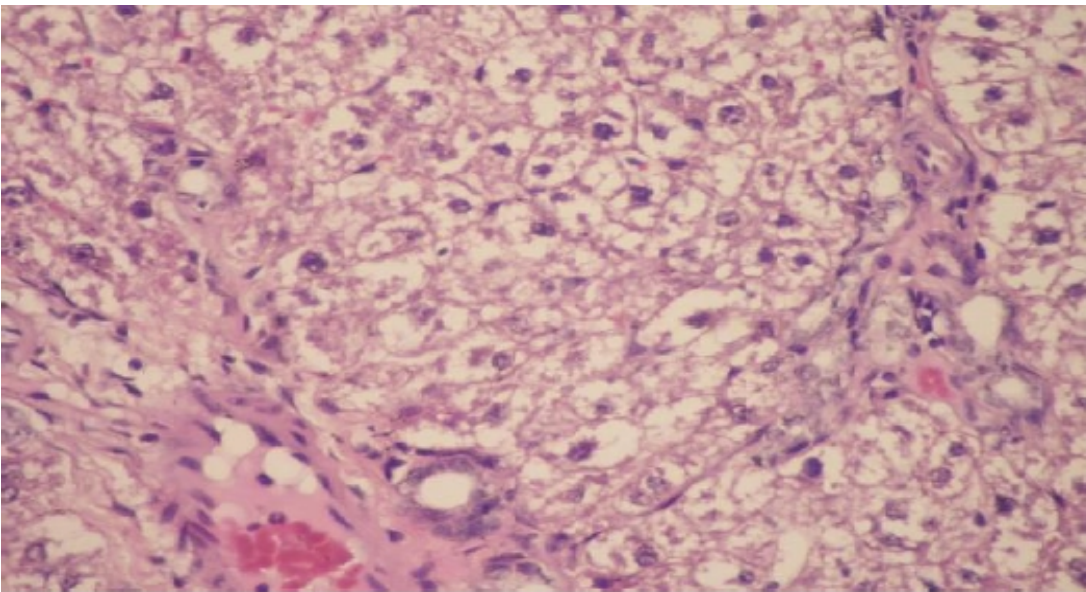
Fig(12): H&E stained hepatic tissue section showing minimal portal inflammation and congestion with apoptotic hepatocytes (arrows). (X400)(100nm after 21 day)



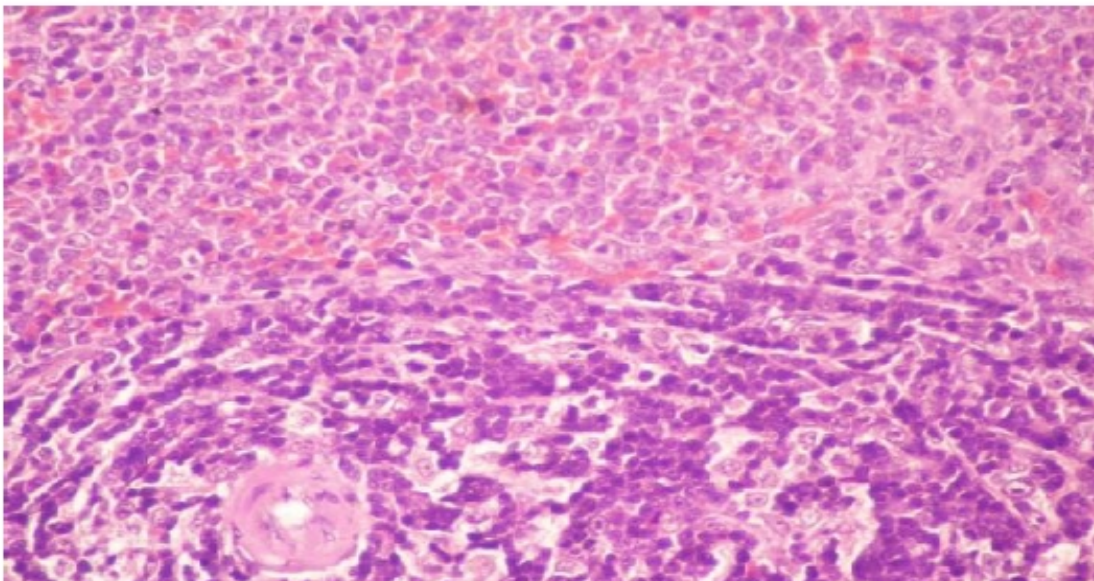
Fig(13): H&E stained hepatic tissue section showing intralobular inflammatory infiltrate with lytic necrosis and Councilman apoptotic bodies (arrows).(X400)(50mn after21 day)



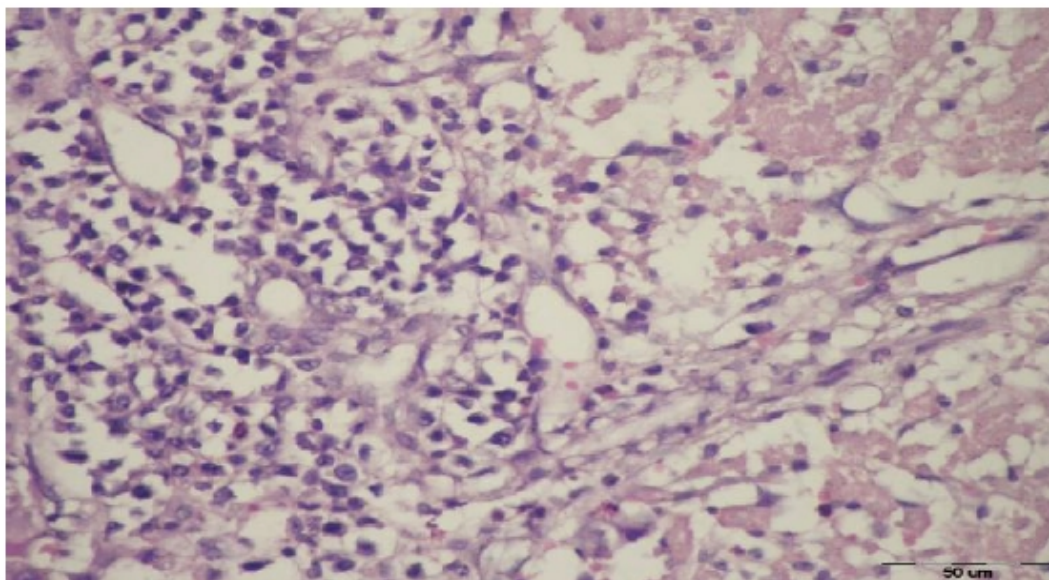
Fig(14): H&E stained hepatic tissue section showing heavy portal inflammation and an apoptotic hepatocyte (arrow)(100nm after 30 min)



Fig(15):H&E stained hepatic tissue section showing early portal fibrosis with short septae (arrows), feathery degeneration of hepatocytes. (X400)(50nm after30 day)



Fig(16): H&E stained splenic tissue section showing reactive white pulp with wide marginal zone. The central arteriole has thick hyalinized wall (arrow). (X400) (50nm after40 day)



Fig(17): H&E stained hepatic tissue section showing moderate portal inflammation, with necrotic hepatocytes (arrows). (X400) (100nm after 40 days)

5.0 DISCUSSION

Nanotechnology has recently emerged as a promising approach for treatment and diagnosis of a variety of diseases.(36) In order to use GNPs in drug delivery, diagnosis, and treatment, it is essential to characterize the toxicity associated with repeated administration of these molecules. In the present study, the toxicological effects of different sizes of colloidal gold nanoparticles were evaluated by assessment of oxidative stress, antioxidants and liver and splenic cell death (apoptosis or necrosis).

In the present study the size and morphology of GNPs were determined by particle size analyzer (PSA) and transmission electron microscopy (TEM) ⁽³⁷⁾. The results revealed the presence of completely spherical GNPs with smooth surfaces and have sizes of 10nm, 50nm and 100nm.

The aggregation shape parameter (ASP) was significantly higher in studied groups compared to the control group, and the percentage of the increase was directly proportional to the time of administration. In each time interval, the ASP values in the 50nm group were higher than in both the 10nm and 100nm groups.

This study presents aggregation shape parameter (ASP) as a quantitative determination of RBC aggregate morphology, derived from the numerical process of digitized image of RBC aggregates. This provides a useful reference for measuring deviations of RBC aggregate morphology: a rouleaux structure characterizes normal aggregates, while the formation of RBC clusters characterizes disease states. ⁽³⁸⁾

Starting from 21st day, whole blood viscosity was significantly higher in studied groups compared to control group. The results are in agreement with several studies who reported that hyperviscosity syndrome can result from gross increase in plasma viscosity, red cell aggregation, elevated hematocrit, and from increased number of circulating rigid red cells (e.g. sickling disorder) or white cells (hyperleucocytosis).⁽³⁹⁻⁴¹⁾

It is known that the inflammatory response is associated with an acute phase reaction characterized by appearance of an increased leukocyte count, accelerated erythrocyte sedimentation rate(ESR), hyperfibrinogenemia, hypergammaglobulinemia, increased synthesis of C-reactive protein (CRP) and other acute phase proteins. The stimulus for production is likely to be inflammatory cytokines such as interleukin-1, interleukin-6 and tumor necrosis factor (TNF). There is a concept that the acute phase proteins are involved in increased red cell aggregation and sedimentation^(42, 43).

In the present study, the toxicity of GNPs has been investigated at the cellular level. The levels of malondialdehyde (MDA) in liver homogenate were significantly higher in all studied groups compared to the control group. Activity of superoxide dismutase (SOD) and levels of reduced glutathione (GSH), and ratio of reduced glutathione to oxidized glutathione (GSH/GSSG) in liver homogenate were significantly lower in all studied groups compared to the control which may confirm the presence of oxidative stress.

Nanomaterial toxicity can occur through several different mechanisms in the body. The main molecular mechanism of *in vivo* nanotoxicity is the induction of oxidative stress by free radical formation.⁽⁴⁴⁾ Oxidative stress may have a role in the induction or the enhancement of inflammation through upregulation of redox sensitive transcription factors (e.g. Nuclear Factor-κB).(45) Slow clearance and tissue accumulation (storage) of potential free radical producing nanomaterials as well as prevalence of numerous phagocytic cells in the organs of the reticuloendothelial system (RES) makes organs such as the liver and spleen main targets of oxidative stress.⁽⁴⁶⁾

Once generated, free radicals can react with all cellular macromolecules, including lipids and proteins. Protein oxidation, particularly of enzymes, can lead to impairment of their function.⁽⁴⁷⁾ Lipid peroxidation is a free radical chain reaction, which arises from the oxidative conversion of

polyunsaturated fatty acids by $O_2H\cdot$ to lipid peroxides, which in turn can damage biological membranes.(48) MDA level is widely utilized as a marker of lipid peroxidation in states of elevated oxidative stress. Possible mechanisms involved in the elevated lipid peroxidation in hepatic toxicity have been proposed.

First, cellular membranes in the liver are rich in polyunsaturated fatty acids, which are especially sensitive to free radical attack. Second, the liver contains a significant amount of iron ions, which stimulate free radical generation.(49)

GSH is a free radical scavenger and a proton donor for glutathione peroxidase. It was reported that depletion of GSH, decreasing GSH to GSSG ratio and decreased glutathione redox potential (ΔEG) are markers of oxidative stress.(50, 51) Our present results were confirmed in accordance with those of Siddiqi *et al* (52) who demonstrated that GNPs cause generation of oxidative stress and an impairment of the antioxidant enzyme glutathione peroxidase in rat brain. GNPs also cause generation of 8-hydroxydeoxyguanosine (8OHdG), caspase-3 and heat shock protein70 (Hsp70), and which may lead to inflammation and DNA damage/cell death.

It was demonstrated that the total GNPs content in cells increased in a time-dependent manner without reaching a plateau in the first 24 h. GNPs were shown to damage the cytoskeleton organization, with the most prominent effect seen for GNPs with size 5 nm.(53)

The results revealed that, the levels of TNF- α in plasma and liver homogenate were significantly higher in all studied groups compared to the control group. These results are in agreement with the other studies which found that, TNF- α levels were elevated in rats with liver injury. Hepatocytes carry receptors that respond even to low TNF- α concentration. Thus, hepatocytes are naturally sensitive to the cytokines. The interaction of TNF- α and TNF- α receptors initiate chemical processes in the cell that lead to apoptosis.(54, 55)

Increased levels of TNF- α in plasma and liver homogenate may be also due to identification of GNPs as foreign by the immune cells, causing the cells to react against either surface or core components to mount an inflammatory response, which involve secretion of signaling molecules to attract more cells to destroy the foreign substances.(54)

Histopathological studies of the hepatic tissue sections of studied animals revealed various degrees of hepatic tissue injury after the four time intervals of the experiment, characterized by mild to heavy portal and lobular inflammation, hepatocellular degeneration, fatty changes (steatosis), apoptosis and necrotic foci which were often associated with fibrosis. On the other hand, the splenic tissue sections of GNPs-administrated rats revealed no significant differences in histology after 14 and 21 days of GNPs administration. While, some morphological changes that include congested red pulp, reactive white pulp and wide reactive marginal zone were observed after 30 and 40 days of GNPs administration.

It was noticed that the recorded abnormal morphological changes in both the hepatic and splenic tissue sections

increased with increasing time of administration. In each time interval, the recorded destructive and degenerative changes were maximum at 50nm GNPs administrated rats. Cho *et al*. (56) studied the *in vivo* toxic effects of 13 nm size PEG-coated GNPs on mice. The nanoparticles were seen to induce acute inflammation and apoptosis in the liver. They accumulated in the liver and spleen for up to 7 days after injection and had long blood circulation times. In addition, transmission electron microscopically examinations revealed that numerous cytoplasmic vesicles and lysosomes of liver Kupffer cells and spleen macrophages contained the PEG-coated gold nanoparticles. Because PEG-coated GNPs are widely used in biomedical applications these effects have obvious clinical implications.

It is thought that nanoparticles should have final hydrodynamic diameters ≤ 5.5 nm to be excreted from the rat body by the renal route. (57) Since the majority of the studied gold nanoparticles are larger than this renal filtration cutoff, in the few studies that have been performed, the gold nanoparticles (NPs) were not excreted in urine; instead they were found to be eliminated from the blood by the reticuloendothelial system (RES) and thus to accumulate in the spleen and liver.(58, 59)

The percentages of the change in all studied parameters were directly proportional to the time of administration. In each time interval, the percentages of the decrease in 50nm group were higher than in both 10nm group and 100nm group. These results are in agreement with the finding of Hyllier and Albertch,(60) who showed that administrated GNPs appeared in various tissues in mice and that the amount of absorption and distribution in the blood was in correlated with the size of the particles.

In most studies, systemically administrated NPs were primarily taken up by liver and spleen in a large quantity and small amounts distributed in the lung, kidney, heart, and brain after single administration. However, little is known about biodistribution, accumulation and toxicity of GNPs after repeated administration.(61-63) Accumulation of nanomaterials in the liver and spleen after being taken up by the reticuloendothelial system could lead to hepatic and splenic toxicity.(64)

In the present histopathological findings, two processes played a role in hepatocyte destruction— apoptosis and necrosis. When a cell undergoes apoptosis, the entire cell, including the nucleus, separates into numerous fragments (i.e., apoptotic bodies).

Simultaneously, the genetic material (i.e., DNA) of apoptotic cells breaks into a characteristic pattern of pieces of varying sizes. During the breakup of the cell, the cell continues to produce proteins and adenosine triphosphate (ATP), a molecule that is required for most of the cell's energy-consuming metabolic processes and which is essential for cell functioning. As a result, each apoptotic body, which is surrounded by a piece of cell membrane, contains intact functional cell components.(65, 66)

6.0 CONCLUSION

In conclusion, the results of *in vivo* cytotoxicity of size-sorted GNPs are the induction of oxidative stress and immune

response. The toxicological effects of GNPs are size and time dependent. Different sizes of GNPs could be endocytosed by hepatic and splenic cells and have large toxic effect on hepatic tissue(apoptosis and necrosis) while its effect on splenic tissue is limited and could be observed after long-term of repeated administration.

7.0 RECOMMENDATIONS

According to the results of our study we recommend the following:

- Avoiding direct exposure to GNPs during their preparation .
- Investigation of the toxicological influence of different sizes and other different properties of GNPs on different tissues such as kidney, brain and lungs.
- Administration of antioxidants before treatment with GNPs in a trial to minimize the toxicological effects of GNPs.

8.0 ACKNOWLEDGEMENTS

The authors are grateful to the animal house of the Medical Research Institute, Alexandria University, Egypt for providing us with the animals used in this study.

9.0 REFERENCES

1. G.K.Stylios, P.V.Giannoudis, T. Wan. Applications of nanotechnology in medical practice. *Injury*. 36, 6(2005).
2. V.Balzani, Nanoscience and nanotechnology: A personal view of a chemist. *Small*.1, 278(2005).
3. R.Sperling, P. Gil, F. Zhang , M.Zanella, W.Parak. Biological applications of gold nanoparticles. *Chem. Soc. Rev.* 37, 1896(2008).
4. M.Grzelczak, J. Pérez-Juste, P.Mulvaney, L. Liz-Marzán. Shape Control in Gold Nanoparticle Synthesis. *Chem. Soc. Rev.* 37,1783(2008).
5. D.T.Felson, J.J. Anderson, R.F.Meenan. The comparative efficacy and toxicity of second-line drugs in rheumatoid arthritis. Results of two meta-analyses. *Arthritis Rheum.* 33,1449(1990)
6. I.C. Shaw. Gold-based therapeutic agents. *Chem Rev.* 99, 2589(1999).
7. K.Unfried, C. Albrecht, L.O. Klotz, A.Von Mikecz, S, Grether-Beck, R.P..FSchins. Cellular responses to nanoparticles: target structures and mechanisms. *Nanotoxicology*. 1,52(2007).
8. Y. Pan, A.Leifert, D.Ruau, S.Neuss, J.Bornemann et al. Gold nanoparticles of diameter 1.4 nm trigger necrosis by oxidative stress and mitochondrial damage. *Small*.5, 2067 (2009).
9. P. Ionita, M. Conte, B. C. Gilbert, V.Chechik Gold nanoparticle-initiated free radical oxidations and halogen abstraction. *Org. Biomol. Chem.* 5, 3504(2007)
10. D. Brown. Calcium and ROS-mediated activation of transcription factors and TNF-alpha cytokine gene expression in macrophages exposed to ultrafine particles, *Am J Physiol Lung Cell Mol Physiol*.286,344 (2004).
11. L.Risom. Acute hypoxia and reoxygenation-induced DNA oxidation in human mononuclear blood cells. *Mutat Res*.625, 125(2007).
12. C.Sioutas, R.J.Delfino, M. Singh. Exposure assessment for atmospheric ultrafine particles (UFPs) and implications in epidemiologic research, *Environ Health Perspect*.113,947 (2005).
13. V. Stone, M.Tuinman, J.E.Vamvakopoulos, J. Shaw, D.Brown et al. Increased calcium influx in a monocytic cell line on exposure to ultrafine carbon black. *EurRespir J.* 15, 297(2000)
14. G.Waris, H.Ahsan. Reactive oxygen species: role in the development of cancer *Carcinog.* 5, 14 (2006).
15. A. Slater, I. Nobel, S.Orrenius. The role of intracellular oxidants in apoptosis. *Biochem. Biophys. Acta*.1271,59(1995)
16. Dumont, S.P.Hehner, T.G.Hofmann et al. Hydrogen peroxide induced-apoptosis is CD95- independent, requires the release of mitochondria-derived reactive oxygen species and the activation of NF-kB. *Oncogene.* 18,747 (1999)
17. E.C. Opera. Oxidative stress. *Dis. Mon.*52, 183(2006)
18. J.Mcdermott. Antioxidant nutrients: current dietary recommendations and research update. *J Am Pharm assoc.*40, 785(2000)
19. J.A.Tainer, E.D.Getzoff, J.S. Richardson, D.C. Richardson. Structure and mechanism of copper, zinc superoxide dismutase. *Nature*.306 , 284(1983)
20. A.Pompella. The changing faces of glutathione, a cellular protagonist. *Biochemical Pharmacology.* 66, 1499(2003)
21. T. Toshiyuki, T.Takahito. Carnosic acid and carnosol inhibit adipocyte differentiation in mouse 3T3-L1 cells through induction of phase2 enzymes and activation of glutathione metabolism. *Biochem. Biophys. Res. Commun.* 382, 549(2009).
22. A.D. McFarland et al. Color My Nanoworld. *J. Chem. Educ.*81, 544A(2004).
23. S.Peng, Y. Lee, C.Wang, H. Yin, S. Dai, S. Sun.A Facile Synthesis of Monodisperse Au Nanoparticles and Their Catalysis of CO Oxidation. *Nano Res.*1, 229 (2008).
24. N. Nguyen, V. Le, D. Chu, C.Sai, T.Cao et al. Synthesis and optical properties of colloidal gold nanoparticles. *J. Phys.*187,12(2009).
25. H.Yazid, R. Adnan, S.Abdulhamid, M.Farrukh. Synthesis and characterization of gold nanoparticles supported on zinc oxide via the deposition-precipitation method. *Turk J Chem.*34,639(2010).
26. M.Elbelbese. Biophysical behavior of red blood cells aggregation under different shear rates. PhD. Thesis submitted to Biophysics Department, Medical Research Institute, Alexandria. *Egypt*.12, 44(2005).
27. M. David, B. Shelly, S. Mark, T. Albert. Hematocrit, Volume exposure, Temperature, and Shear Rate Effects on Blood viscosity. *Anesth Analg.* 91,539(2000).
28. H.H. Draper, M. Hadley. Malondialdehyde determination as index of lipid peroxidation. *Methods Enzy mol.*186, 421(1990).
29. S. G.Marklund. Involvement of superoxide anion radical in autoxidation of pyrogallol and a convenient assay for SOD. *Eur. J. Biochem.*47, 469(1974).
30. O.W. Griffith. Determination of glutathione and glutathione disulfide using glutathione reductase and 2-vinyl pyridine. *Anal Biochem.*106,207 (1980).

31. F. Q. Schafer, G FBuettner. Redox environment of the cell as viewed through the redox state of the glutathione disulfide . glutathione couple. *Free Radic Biol Med.*30,1191.(2001).
32. O.H. Lowry, N.J.Rosebrough, A.L. Farr, R.J. Randall. Protein measurements with Folin-phenol reagent. *J. Biol. Chem.* 193,265(1951).
33. J.I.Y. Chung, E.N.Benveniste. Cloning and sequence analysis of the rat tumor necrosis factor –encoding genes. *Gene.*132,227 (1993).
34. J.D. Bancroft, A.Stevans, D.R.Tuener. (1996): Theory and Practice of Histopathological Techniques", 4th ed., Churchill Livingstone, Edinburgh, London, Melbourne, New York
35. M.J.Nursis. Statistical package for social sciences for the IBMPC / XT: statistical guide, ver. 11.5.0. Chicago, Illinois: SPSS Inc.; 2002.
36. S.D. Caruthers, SA Wickline, GMLanza. Nanotechnological applications in medicine. *Curr. Opin. Biotechnol.* 18,26(2007).
37. A.D.McFarland and C.L. Haynes. Color My Nanoworld. *J. Chem. Educ.* 81,544A(2004).
38. S. Chen. Monitoring of erythrocyte aggregate morphology under flow by computerized image analysis. *Biorheology.*32,487(1995)
39. J. Fahey, W Barth, A. Solomon. Serum hyperviscosity syndrome.*J.A.M.A.* 192,464(1965).
40. M.K.Home. Sickle cell anemia as a rheologic disease. *Amer. J .Med.*..70,288 (1981).
41. M.Lichtman, J. Row. Hyperleukocytic leukemias: Rheological, clinical and therapeutic considerations blood. 60, 279(1982).
42. S.E. Epstein, Y.F. Zhou, J. Zhu. Infection and atherosclerosis: emerging mechanistic paradigms. *Circulation.*100,20 (1999).
43. X.Weng, G. Cloutier, R. Beaulieu, et al. Influence of acute-phase proteins on erythrocyte aggregation. *Am J Physiol.*..271,2346(1996).
44. S.Lanone, J.Boczkowski. Biomedical applications and potential health risks of nanomaterials: molecular mechanisms. *CurrMol Med.* 6,651(2006).
45. I.Rahman. Regulation of nuclear factor- κ B, activator protein-1, and glutathione levels by tumor necrosis factor- α and dexamethasone in alveolar epithelial cells. *Biochem Pharmacol.*60,1041(2000).
46. I. Rahman, S.K.Biswas, L.A.Jimenez, M. Torres, H.J.Forman. Glutathione, stress responses, and redox signaling in lung inflammation. *Antioxid Redox Signal.*7, 42(2005)
47. A. Cherubini, C.Polidori, C. Benedetti, S.Ercolani, U.Senin, P.Mecocci. Association Between Ischemic Stroke and Increased Oxidative Stress. *Stroke.*28,2231(2002).
48. A.Yildirim, M.Gumus, S.Dalga, Y.N.Sahin, F.Akca. Dehydroepiandrosterone improves hepatic antioxidant systems after renal ischemia-reperfusion injury in rabbits. *Ann Clin Lab Sci.* 33, 459(2003).
49. S.M.H.Sadrzadeh, A.A.Nanji, .PL. Price. The oral iron chelator, 1,2-dimethyl-3- hydroxypyrid-4-one reduces hepatic free iron, lipid peroxidation and fat accumulation in chronically ethanol-fed rats. *Journal of Pharmacology and Experimental Therapies.*269,632 (1994).
50. J.B. Schulz, J.Lindenau, J.Seyfried, J.Dichgans. Glutathione, oxidative stress and neurodegeneration.*Eur J Biochem .* 267, 4904 (2000)
51. D.S. Warner, H, Sheng IBatinic-Haberle. Oxidants, antioxidants and the ischemic brain.*J Exp Biol.* 207, 3221(2004).
52. J.N.Siddiqi,A.K. M.Abdelhalim,A. K. El-Ansary,S.A.Alhomida, W.Y.Ong. Identification of potential biomarkers of gold nanoparticle toxicity in rat brains. *J Neuroinflammation.*9,123(2012).
53. C. P.Gioria, P.García, F.Nativo, D.Franchin, J. Gilliland, F.Ponti.In "Toxicology Letters" .11,22(2012).
54. C.J.McClain, D.A. Cohen, C.A.Dinarello, J.G. Cannon, S.I .Shedlofskyet al. Cytokines and alcoholic liver disease.*Seminars in Liver Disease.* 13,170.(1993).
55. J.Ghos, J. Das, P .Manna, P.C.Sil. Acetaminophen induced renal injury via oxidative stress andTNF-alpha production: Therapeutic potential of arjunolic acid. *Toxicology.*268, 8 (2010).
56. W.S. Cho, M. Cho, J.Jeong, M.Choi, H.Y.Cho, B.S.Han, S.H. Kim, H.O. Kim, Y.T.Limc, B.H. Chung, J.Jeong. Acute toxicity and pharmacokinetics of 13 nm-sized PEG-coated gold nanoparticles. *Toxicol Appl Pharmacol.* 236,16(2009).
57. H.S. Choi, J.P. Zimmer, E. Tanaka, J.V.Frangioni, I. M.Bawendet al. Renal clearance of quantum dots. *Nat Biotechnol.*25,1165(2007)
58. W.H. De Jong, W.I.Hagens, P.Krystek, R.MCBurge, A.J.A.M.Sips, R.E.Geertsma. Particle sizedependent organ distribution of gold nanoparticles after intravenous administration. *Biomaterials.*29,1912(2008).
59. G.Von Maltzahnji-Ho ParkA.Agrawal, N. K.Bandaru, S. K. DasM. J. Sailor,S. N. Bhatia.Computationally guided photothermal tumor therapy using long circulating gold nanorod antennas. *Cancer Res.*69,3892(2009)
60. J.F.Hillyer, R.M.Albrecht. Gastrointestinal persorption and tissue distribution of differently sized colloidal gold nanoparticles. *J. Pharm. Sci.* 90,1927(2001).
61. G.Sonavane, K.Tomoda, K. Makino.Biodistribution of colloidal gold nanoparticles after intravenous administration: effect of particle size. *Colloids Surf. B Biointerfaces.*66 ,274(2008)
62. W.H. De Jong, W.I.Hagens, P.Krystek, M.C. Burger, A.J.Sips et al. Particle size-dependent organ distribution of gold nanoparticles after intravenous administration. *Biomaterials .* 29,1912(2008)
63. M.Semmler-Behnke, W.G.Kreyling, J.Lipka, S.Fertsch, A.Wenk, S.Takenaka et al. Biodistribution of 1.4- and 18-nm gold particles in rats, *Small .*4,2108(2008)
64. Y.S. Chen, Y.C. Hung, I.Liau, G.S. Huang. Assessment of the in vivo toxicity of gold nanoparticles.*Nanoscale Res Lett.* 4,858(2009)
65. B.I.Jugdutt, H.A.Idikio. Apoptosis and oncosis in acute coronary syndromes: Assessment and implications. *Mol Cell Biochem.* 270, 177(2005)
66. B.G. Rosser, G.J.Gores. Liver cell necrosis: Cellular mechanisms and clinical implications. *Gastroenterology.* 108,252(1995)